Realization of Localized Bohr-Like Wave Packets

J. J. Mestayer,[1] B. Wyker,[1] J. C. Lancaster,[1] F. B. Dunning,[1] C. O. Reinhold,[2,3] S. Yoshida,[4] and J. Burgdörfer[4,3]

[1]*Department of Physics and Astronomy and the Rice Quantum Institute, Rice University, Houston, Texas 77005-1892, USA*

[2]*Physics Division, Oak Ridge National Laboratory, Oak Ridge, Tennessee 37831-6372, USA*

[3]*Department of Physics, University of Tennessee, Knoxville, Tennessee 37996, USA*

[4]*Institute for Theoretical Physics, Vienna University of Technology, Vienna, Austria, EU*

(Received 27 February 2008; published 20 June 2008)

We demonstrate a protocol to create localized wave packets in very-high-n Rydberg states which travel in nearly circular orbits around the nucleus. Although these wave packets slowly dephase and eventually lose their localization, their motion can be monitored over several orbital periods. These wave packets represent the closest analog yet achieved to the original Bohr model of the hydrogen atom, i.e., an electron in a circular classical orbit around the nucleus. The possible extension of the approach to create ''planetary atoms'' in highly correlated stable multiply excited states is discussed.

DOI: 10.1103/PhysRevLett.100.243004 PACS numbers: 32.80.Qk, 32.60.+i, 32.80.Rm

Highly excited (Rydberg) atoms in nearly circular states are characterized by extremely high values of one component of the angular momentum $\langle L \rangle \sim \pm(n-1)\hbar$, where n is the principal quantum number. Discussion of such states dates back to the first model of the hydrogen atom developed by Bohr and subsequently extended to elliptical states by Wilson and Sommerfeld. With the advent of new experimental techniques, circular Rydberg atoms have received renewed attention. They have numerous potential applications such as in information processing, in cavity quantum electrodynamics, and in precision spectroscopy [1–5]. These rely on the production of stationary circular states for which various techniques have been devised [6–10].

The development of ultrafast electromagnetic pulses opens up the possibility of engineering ''nonstationary'' circular wave packets which resemble a localized quasiclassical electron moving in a Kepler orbit. This goal dates back to early ''gedanken'' experiments by Schrödinger [11], who focused on constructing nondispersive minimum-uncertainty wave packets similar to coherent harmonic oscillator eigenstates. Such schemes failed because, in atoms, the energy levels are not equispaced, leading to dephasing. However, at high n, the energy levels are approximately equispaced, allowing production of wave packets that can remain localized for extended periods [12]. Techniques for producing and probing Rydberg wave packets have become feasible only recently [13–16] using pulses whose time scales are smaller than the electron Kepler period $T_n = 2\pi n^3$ (atomic units are used throughout). However, even transiently localized circular wave packets are difficult to produce experimentally and have been primarily the subject of theoretical work [17,18]. Here we experimentally demonstrate the creation of such wave packets near $n \sim 300$ which behave much as a classical electron in a nearly circular Kepler orbit. The motion of the wave packets can be followed for several Kepler periods and provides a direct analog of the original Bohr atom. Such Bohr-like wave packets could represent an important stepping stone towards realization of phase-locked correlated planetary configurations in multielectron atoms [19–21].

The present protocol employs atoms with $n \sim 300$ having radii $r \sim n^2 \sim 5$ μm, binding energies $E = -1/(2n^2)$ in the sub-meV regime, and classical electron orbital periods $T_n \sim 4.4$ ns. Initially, very-high-n potassium Rydberg atoms are created by photoexciting the lowest-lying states in the $n = 306$ Stark manifold in the presence of a weak ($F_x^{\rm dc} \sim 500$ μV cm^{-1}) dc field directed along the x axis. Because of Doppler broadening, the excited atoms are a stationary statistical mixture of ~36 Stark states. These states are quasi-one-dimensional (quasi-1D) and are oriented along the x axis [16,22]. A much larger dc field $F_z^{\rm pump} \sim -20$ mV cm^{-1} is then suddenly (rise time $\ll T_n$) applied along the z axis. This transverse field creates a nonstationary Stark wave packet comprising a coherent superposition of Stark states (defined along $F_z^{\rm pump}$) having a narrow range of n ($\Delta n \sim 24$). Figure 1 shows a typical classical trajectory of an electron in a highly elliptical orbit oriented along the x axis when suddenly exposed to $F_z^{\rm pump}$. Its orbit begins to precess, undergoing periodic changes from a highly elliptic to a nearly circular trajectory and back on the time scale of the Stark precession period $T_S \sim 2\pi/(3|F_z^{\rm pump}|n) \sim 43$ ns. Because the Heisenberg quantum break time $\tau_H \propto n^4$, beyond which classical and quantum dynamics diverge, is in the microsecond regime for $n \sim 300$ [16], the present protocol is discussed using classical dynamics.

Since the electron motion is (approximately) confined to the xz plane, the oscillations in eccentricity lead to periodic variations in the y component of angular momentum L_y, as shown in the inset in Fig. 1. These results were calculated by using the classical trajectory Monte Carlo (CTMC) approach. A microcanonical ensemble of points in phase space is used to represent the initial mix of Stark states, and the time evolution of the wave packet, i.e., of the ensemble

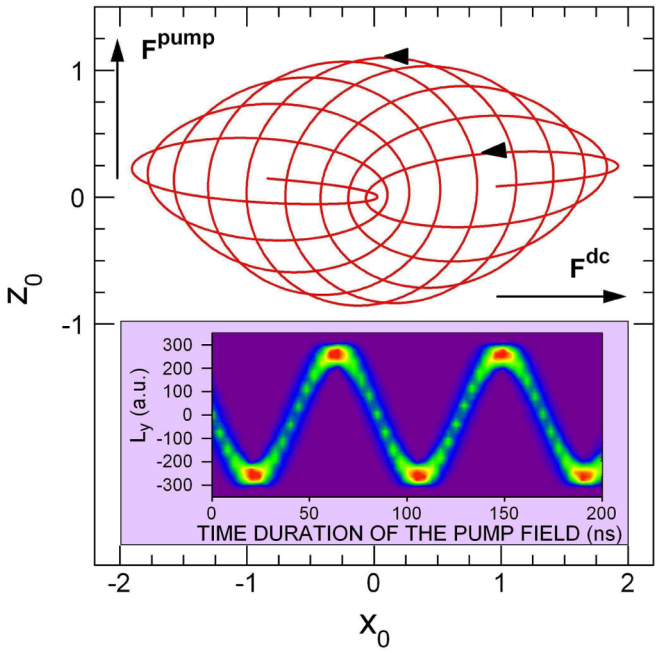

FIG. 1 (color online). Time evolution of a classical Rydberg electron trajectory ($n_i = 306$) in a field $F_z^{\text{pump}} = -20$ mV cm^{-1} directed along the z axis. The electron orbit is initially oriented along the x axis, and the motion, projected into the xz plane, is followed for one Stark precession period $T_S \sim 43$ ns. Inset: Calculated evolution of the distribution in the y component of angular momentum L_y for the wave packet. Scaled units $x_0 = x/n_i^2$ and $z_0 = z/n_i^2$ are used.

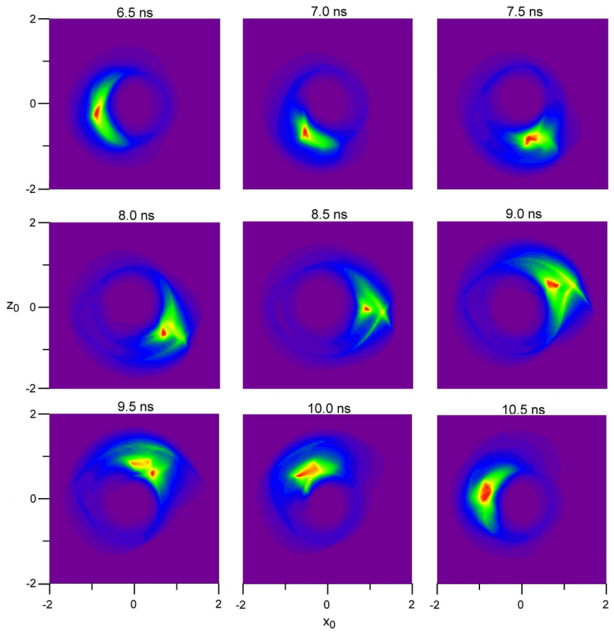

FIG. 2 (color online). Snapshots showing the evolution of the simulated wave packet following application of a pump field $F_z^{\text{pump}} = -20$ mV cm^{-1} for 22 ns to quasi-1D $n_i = 306$ atoms. These are taken at the times shown after turn-off of F_z^{pump} and represent projections on the xz plane. Scaled units $x_0 = x/n_i^2$ and $z_0 = z/n_i^2$ are used.

of points, is followed by solving Hamilton's equation of motion for each initial point. In the presence of the pump field F_z^{pump}, the distribution in L_y remains narrow and oscillates sinusoidally, periodically becoming strongly peaked at values of $L_y \sim -270$ (or $+270$) ± 35, which corresponds to an electron traveling anticlockwise (or clockwise) around a nearly circular orbit. Switching off the pump field at such times "freezes" the L_y distribution, leaving the atom in a nearly circular state. This operation is similar to the "$\pi/2$ pulse" used to manipulate nuclear spins [23] and to a theoretical proposal to produce stationary circular states [9,24].

Figure 2 shows snapshots of the simulated wave packet resulting from application of a field F_z^{pump} that is turned off after 22 ns ($\sim T_S/2$), i.e., when L_y reaches its largest negative value. A localized wave packet is evident that moves in a nearly circular orbit. As seen in Fig. 3, which shows the time evolution of the electron distribution in both angle and radius, the wave packet remains well localized for several orbits. It circulates with near constant radius ($\sim n^2$) and, since its angular position depends linearly on time, with constant angular velocity and momentum ($\sim n^{-1}$). The localization of the wave packet in azimuth initially improves with time becoming optimum $\sim$7–12 ns after turn-off of the pump field, when its full width half maximum amounts to $\sim$1 radian. (The first snapshot in Fig. 2 is taken $\sim$7 ns after the field is turned off.) The coordinate of the wave packet moves in an approximately circular orbit with angular frequency $\omega_n = n^{-3}$ given by

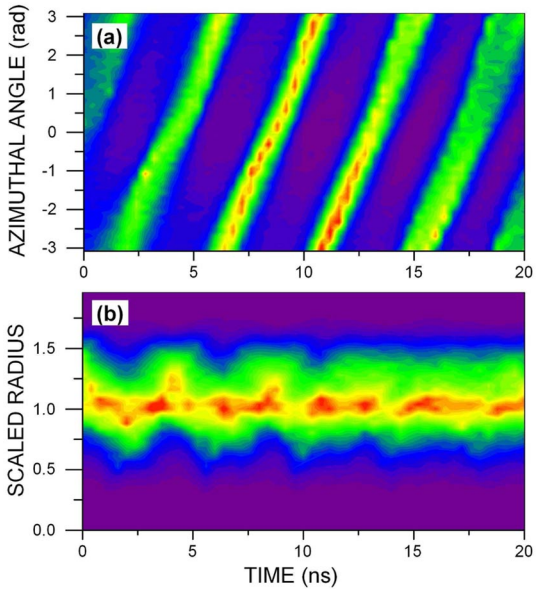

FIG. 3 (color online). Time dependence of (a) the angular and (b) the radial distributions of the wave packet following turn-off of a pump field of -20 mV cm^{-1} applied for 22 ns. The azimuthal angles are measured from the $+x$ axis. Scaled units $r_0 = r/n_i^2$ are used.

$$(x(t), z(t)) \simeq n^2(\cos(\omega_n t + \delta), \sin(\omega_n t + \delta)), \quad (1)$$

where δ is constant phase shift. The momentum components

$$(p_x(t), p_z(t)) \simeq n^{-1}(-\sin(\omega_n t + \delta), \cos(\omega_n t + \delta)) \quad (2)$$

are 90° out of phase with the spatial coordinates. The expectation values of these quantities [Figs. 4(a) and 4(b)] closely mirror Eqs. (1) and (2). The y coordinate and its expectation value remain close to zero, consistent with motion in the xz plane, while strong oscillations are observed for $\langle x\rangle$, $\langle z\rangle$, $\langle p_x\rangle$, and $\langle p_z\rangle$

To experimentally test these predictions, quasi-1D Rydberg atoms oriented along the x axis were first formed by using an extra-cavity doubled CR699-21 Rh6G dye laser to photoexcite potassium atoms contained in a thermal-energy beam to a mix of the lowest-lying red-shifted states in the $n_i = 306$ Stark manifold in a weak ($\sim$500 μV cm^{-1}) dc field directed along the x axis (see

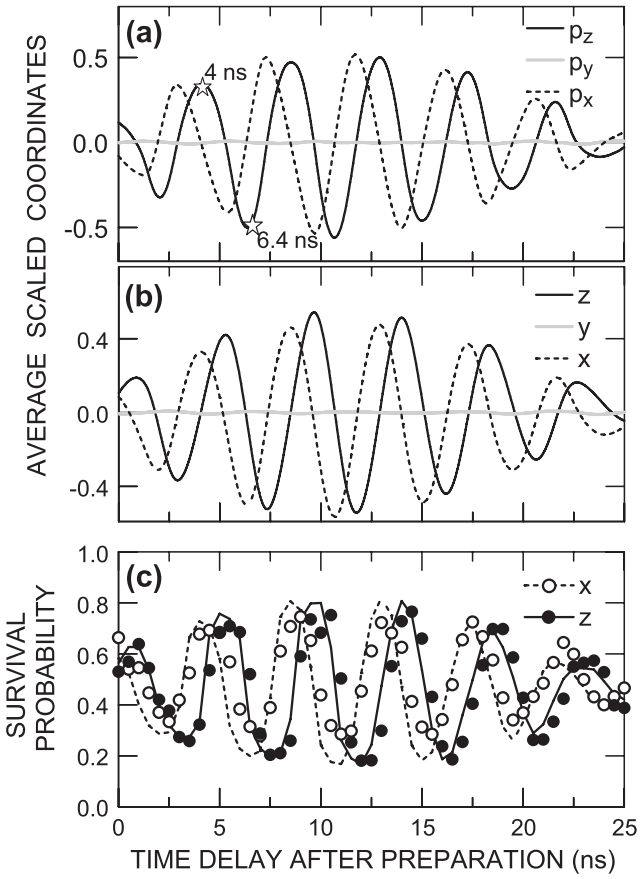

FIG. 4. Time dependence of (a) the momentum coordinates, (b) the position coordinates, and (c) the experimental (symbols) and calculated (lines) survival probabilities following turn-off of a pump field $F_z^{\text{pump}} = -20$ mV cm^{-1} applied for 22 ns. The probe pulses used for (c) were of 6 ns duration and amplitude -100 mV cm^{-1} directed along the x and z axes (see text). Scaled units, e.g., $x_0 = x/n_i^2$ and $p_{x0} = n_i p_x$, are used. The stars in (a) indicate the times at which the momentum is probed in Fig. 5.

[16,22] for details). The pump field of -20 mV cm^{-1} was then suddenly applied (rise time $\sim$0.3 ns) in the z direction. After a predetermined time, this field was rapidly turned off (fall time $\sim$0.3 ns). The subsequent behavior of the wave packet was monitored by using probe pulses applied along the x or z axes. The number of surviving atoms, and thus the survival probability, was determined by field ionization.

Applying a "field step" at $t = t_p$, i.e., suddenly turning on a constant field, indirectly probes the electron position coordinates by ionizing those electrons whose coordinates $z(t_p)$ [or $x(t_p)$] are such that their energy $-1/(2n^2) + z(t_p)F_z^{\text{probe}}$ [or $-1/(2n^2) + x(t_p)F_x^{\text{probe}}$] lies above the top of the barrier ($-2|F^{\text{probe}}|^{1/2}$) generated by the probe pulse [25]. By using a probe field of -100 mV cm^{-1} and a duration of 6 ns ($>T_n$), strong periodic oscillations in survival probability are observed [Fig. 4(c)], which follow $\langle x(t)\rangle$ and $\langle z(t)\rangle$ and are in excellent agreement with CTMC simulations. These results confirm the production of a localized wave packet in a nearly circular orbit around the core ion. Oscillations persist for several orbits but ultimately dephase due to the distribution of excited states in the wave packet ($n \sim 306 \pm 12$).

Further evidence of nearly circular motion is obtained by probing the momentum of the wave packet by applying a very-short-pulsed unidirectional field, termed a half-cycle pulse, directed along the z axis (duration $\sim$0.8 ns $\ll T_n$). In this limit, a pulse $F_z^{\text{probe}}(t)$ centered at $t = t_p$ simply delivers an impulsive momentum transfer or a "kick" $\Delta p = -\int F_z^{\text{probe}}(t)dt$ to the excited electron. Measurements of the ensuing survival probabilities are shown in Fig. 5 as a function of Δp. When the electron is located on the $+x$ axis moving in the $+z$ direction, a kick Δp in the $+z$ direction will accelerate the electron and increase its energy. Even relatively small kicks can lead to ionization. In contrast, if the electron is located on the $-x$ axis traveling in the $-z$ direction, small kicks will tend to decelerate the electron and reduce its energy leading to stronger binding. Only if the kick is strong enough to accelerate it in the reverse direction will the electron gain energy admitting the possibility for ionization. In consequence, much larger kicks are required to induce ionization. Pronounced differences in the survival probabilities are evident in Fig. 5 that agree well with the results of CTMC simulations. Measurements of the survival probability as Δp is varied provide not only the expectation value $\langle p_z\rangle$ but also information on the distribution of p_z [15,25].

Measurements (not shown) were also undertaken in which the pump field was turned off at $t \sim 65$ ns and confirmed production of a localized wave packet that rotated clockwise in the xz plane with $L_y \sim 270$. Further work is under way to optimize the present wave packets by varying the strength, duration, and the rise and fall times of the pump pulse. These parameters promise control of the

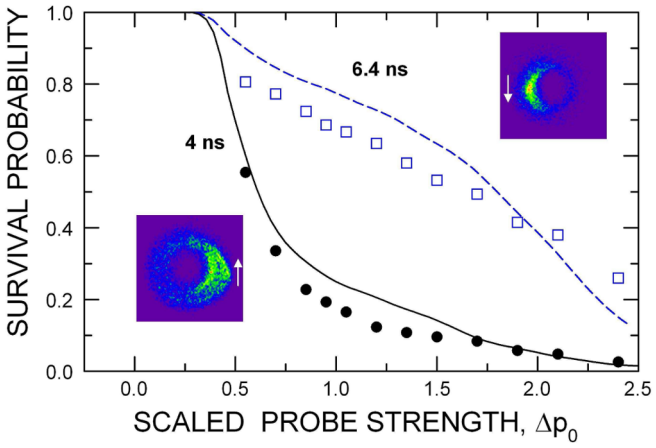

FIG. 5 (color online). Survival probabilities versus the strength $|\Delta p|$ of a probe half-cycle pulse (expressed in scaled units $\Delta p_0 = n_i \Delta p$) applied in the $+z$ direction when the electron is on the $+x$ axis moving in the $+z$ direction (4 ns) and on the $-x$ axis moving in the $-z$ direction (6.4 ns). The dc field parameters used are as in Fig. 3. Symbols, experimental data; lines, results of CTMC simulations.

initial wave packet localization and of the distribution of final n levels in the wave packet.

The production of Bohr-like wave packets opens up exciting opportunities to engineer ''planetary atoms'' [19,21,26,27] containing two excited electrons far from the ground state, including frozen planetary states [28]. In planetary two-electron wave packets, the ''outer'' electron (as it rotates in its circular orbit) can polarize the orbit of the ''inner'' electron creating a dipole that revolves in lockstep with the outer electron [29]. Such correlated motion can lead to long-term stability against radiative decay and autoionization. Good candidates for these double Rydberg states are the alkaline earths for which stepwise ''isolated core'' excitation of a second, inner electron has been successfully demonstrated [30]. The present $n \sim 300$ circular wave packets would be an excellent starting point for such excitation (coupling to the core is extremely weak, and the orbital period $\sim$4.4 ns is sufficiently long that phase selective excitation of an inner electron should be feasible with current laser technology.) Preliminary simulations indicate that phase-correlated collective two-electron motion resembling that in Ref. [29] can be achieved for a broad range of principal quantum numbers n_{in} of the inner electron $(60 < n_{\text{in}} < 130)$. Clearly, however, realization of this protocol poses considerable experimental challenges.

This research was supported by the NSF under Grant No. 0650732, the Robert A. Welch Foundation under Grant No. C-0734, the OBES, U.S. DOE to ORNL, which is managed by the UT-Batelle LLC under Contract No. AC05-00OR22725, and the FWF (Austria) under No. SFB016.

[1] S. Gleyzes *et al.*, Nature (London) **446**, 297 (2007).
[2] M. Brune *et al.*, Phys. Rev. Lett. **76**, 1800 (1996).
[3] E. Hagley *et al.*, Phys. Rev. Lett. **79**, 1 (1997).
[4] M. Gross and J. Liang, Phys. Rev. Lett. **57**, 3160 (1986).
[5] A. Nussenzweig *et al.*, Europhys. Lett. **14**, 755 (1991).
[6] C. H. Cheng, C. Y. Lee, and T. F. Gallagher, Phys. Rev. Lett. **73**, 3078 (1994).
[7] J. C. Day *et al.*, Phys. Rev. Lett. **72**, 1612 (1994).
[8] J. Hare, M. Gross, and P. Goy, Phys. Rev. Lett. **61**, 1938 (1988).
[9] R. Lutwak *et al.*, Phys. Rev. A **56**, 1443 (1997).
[10] D. Delande and J. C. Gay, Europhys. Lett. **5**, 303 (1988).
[11] E. Schrödinger, Naturwissenschaften **14**, 664 (1926).
[12] L. S. Brown, Am. J. Phys. **41**, 525 (1973).
[13] J. A. Yeazell and C. R. Stroud, Phys. Rev. Lett. **60**, 1494 (1988).
[14] A. ten Wolde *et al.*, Phys. Rev. Lett. **61**, 2099 (1988).
[15] R. R. Jones and L. Noordam, Adv. At. Mol. Opt. Phys. **38**, 1 (1998).
[16] F. B. Dunning *et al.*, Adv. At. Mol. Opt. Phys. **52**, 49 (2005).
[17] Z. D. Gaeta, M. W. Noel, and C. R. Stroud, Phys. Rev. Lett. **73**, 636 (1994).
[18] I. Bialynicki-Birula, M. Kalinski, and J. H. Eberly, Phys. Rev. Lett. **73**, 1777 (1994).
[19] I. C. Percival, Proc. R. Soc. A **353**, 289 (1977).
[20] G. Tanner, K. Richter, and J.-M. Rost, Rev. Mod. Phys. **72**, 497 (2000).
[21] S. N. Pisharody and R. R. Jones, Science **303**, 813 (2004).
[22] C. L. Stokely *et al.*, Phys. Rev. A **67**, 013403 (2003).
[23] C. P. Slichter, *Principles of Magnetic Resonance* (Springer, New York, 1992).
[24] P. Bellomo and C. R. Stroud, Phys. Rev. A **59**, 2139 (1999).
[25] B. E. Tannian *et al.*, Phys. Rev. A **64**, 021404(R) (2001).
[26] T. Uzer *et al.*, Science **253**, 42 (1991).
[27] A. Buchleitner *et al.*, Phys. Rep. **368**, 409 (2002).
[28] K. Richter and D. Wintgen, J. Phys. B **24**, L565 (1991).
[29] M. Kalinski *et al.*, Phys. Rev. A **67**, 032503 (2003).
[30] U. Eichmann, V. Lange, and W. Sandner, Phys. Rev. Lett. **64**, 274 (1990).